

# Supporting Information

## Benchmark First Principles Calculations of Adsorbate Free Energies

Anshumaan Bajpai,<sup>†,¶</sup> Prateek Mehta,<sup>†,¶</sup> Kurt Frey,<sup>†</sup> Andrew M. Lehmer,<sup>†</sup> and  
William F. Schneider<sup>\*,†,‡</sup>

<sup>†</sup>*Department of Chemical and Biomolecular Engineering, University of Notre Dame, Notre  
Dame, IN 46556, USA*

<sup>‡</sup>*Department of Chemistry and Biochemistry, University of Notre Dame, Notre Dame, IN  
46556, USA*

<sup>¶</sup>*Contributed equally to this work*

E-mail: wschneider@nd.edu

# S1 Adsorbate Specific Contribution to Free Energy

Free energies and entropies of surface adsorbates have a concentration dependence in addition to the non-interacting standard state component computed in the main text. For an ensemble of  $n_A$  adsorbates on a surface of area  $B$  (We use  $B$  to avoid confusion with the Helmholtz energy  $A$ ), the partition function and total free energy are related by

$$A(n_A, B, T) = -k_B T \ln Q(n_A, B, T) \tag{S1}$$

It is conventional to define a surface site of area  $\alpha$ , such that  $B = N\alpha$ , where  $N$  is the number of sites. Because free energy is first-order homogeneous in the extensive variables, this expression can be written as  $A(n_A, N\alpha, T) = Na(n_A/N, T) = Na(\theta, T)$  where  $\theta$  is a dimensionless coverage and  $a$  is free energy per site of (implicit) area  $\alpha$ . By convention, we write

$$a(\theta, T) = a^\circ(T) + (a(\theta, T) - a^\circ(T)) \tag{S2}$$

to separate  $a$  into an adsorbate-specific and a coverage-dependent component. Here we take the standard state to be one adsorbate per site in the ideal (non-interacting) limit and compare all models against the same site size. (Note that it is a separate but reasonable question as to how close the DFT supercells used in this work are to the non-interacting limit. We expect and have found the PES variation with supercell size to be small for the adsorbates and supercells used here. Because of the implications of periodic boundary conditions on adsorbate displacement, however, it would be incorrect to claim that the PES computed within a particular supercell are representative of adsorbates at the concentration implied by that supercell.)

It is common and reasonable to seek to capture the concentration dependence of the free energies as well, and care must be taken in comparing models and to distinguish the subtly different concepts of standard state and normalization. Note that exact computation of the

free energy would require  $Q(n_A, B, T)$  to be evaluated as a function of concentration, and that this type of problem is commonly addressed in the fluids simulation community using empirical potentials and Monte Carlo or molecular dynamics sampling.

In the Langmuir model, each adsorbate is assumed to be identical, non-interacting, to occupy a site of some specific size, and to exclude other adsorbates from the same adsorption site. In this model,  $n_A \leq N$ ,

$$Q(n_A, B, T) = q(T)^{n_A} \frac{N!}{n_A!(N - n_A)!} \quad (\text{S3})$$

and

$$A(n_A, B, T) = -k_B T (n_A \ln q(T) + \ln N! - \ln n_A! - \ln(N - n_A)!) \quad (\text{S4})$$

On applying Stirling's approximation and factoring, we obtain:

$$a(\theta, T) = A/N = -k_B T (\theta \ln q(T) - \theta \ln \theta - (1 - \theta) \ln(1 - \theta)) \quad (\text{S5})$$

Taking the site to be of area  $\alpha$  and taking the limit that  $\theta \rightarrow 1$ ,  $a(\theta, T) = -k_B T \ln q(T)$ , the quantity we report in Figures 4, 5, and 6 for the harmonic oscillator (HO), hindered translator (HT), and ideal gas models as well as for the full solutions. We assume in the HO and full models that wavefunctions vanish at the boundaries of the site, which is equivalent to the assumption that contributions to the free energy of the adsorbate from visiting regions beyond the site are captured in the configurational ( $\theta$ )-dependent part of the free energy. For sufficiently flat (low frequency) HO potentials, low energy wavefunctions can extend beyond the site boundaries, leading to HO free energies unphysically less than the free translator (discussed further in Section 4 of the main text).

The ideal gas model again assumes each adsorbate to be identical and non-interacting, to move on a constant potential energy surface, and, importantly, to occupy zero volume (i.e.,

not to exclude other adsorbates from the same site). In this model we can write

$$Q(n_A, B, T) = \frac{q^{\text{ideal}}(B, T)^{n_A}}{n_A!} \quad (\text{S6})$$

and

$$\begin{aligned} A(n_A, B, T) &= -n_A k_B T \ln q^{\text{ideal}}(B, T) + k_B T \ln n_A! \\ &\approx -n_A k_B T (\ln q^{\text{ideal}}(B, T) - \ln n_A + 1) \end{aligned} \quad (\text{S7})$$

where we again apply Stirling's approximation. Further,

$$q^{\text{ideal}}(B, T) \approx \left( \frac{B}{\Lambda^2} \right) \quad (\text{S8})$$

which derives from an integral approximation on  $q$  and is valid when the linear dimensions are greater than the thermal wavelength,  $\Lambda = h/\sqrt{2\pi m k_B T} \approx 0.3 \text{ \AA}$  at 200 K for an O adsorbate. The integral approximation fails at sufficiently low temperature, as is evident from the incorrect low temperature limiting behavior seen in Figures 4, 5, and 6 (d) in the ideal gas model.  $q^{\text{ideal}}$  is linear in  $B$ . We again take the area of a site to be  $\alpha$  to write the ideal gas free energy normalized to the number of sites as

$$a(\theta, T) = A/N = -k_B T \frac{n_A}{N} \left( \ln q^{\text{ideal}}(T) + \ln(B/\alpha) - \ln n_A + 1 \right) \quad (\text{S9})$$

$$a(\theta, T) = -k_B T \left( \ln q^{\text{ideal}}(T) - \ln \theta + 1 \right) \quad (\text{S10})$$

This construction is valid for any  $\alpha$  large enough such that the linear dimensions are greater than  $\Lambda$ , i.e. as long as translational states of wavelength greater than the box size contribute negligibly to the total number of translational states. In the limit  $\theta \rightarrow 1$ ,  $a(\theta, T) = -k_B T (\ln q^{\text{ideal}}(T) + \ln e)$ , where the  $\ln e$  term emerges from the zero excluded volume assumption. This term diminishes the free energy per site by  $-k_B T$ . As it emerges

from the zero volume assumption and not the local site contribution to the free energy, we plot  $-k_{\text{B}}T \ln q^{\text{ideal}}(T)$  in Figures 4, 5, and 6. Thus, the ideal gas results in these figures corresponds to free particles occupying sites of area  $\alpha$  and excluding other particles from the same site.

Finally, we note that while the free energy and entropy per site vanish in the zero coverage limit, the free energy per adsorbate particle (the adsorbate chemical potential) does not. The adsorbate chemical potentials in the two models are given by

$$\mu^{\text{Langmuir}}(\theta, T) = -k_{\text{B}}T (\ln q - \ln \theta - \ln(1 - \theta)) \quad (\text{S11})$$

and

$$\mu^{\text{ideal}}(\theta, T) = \left( \frac{\partial A(n_A, N, T)}{\partial n_A} \right)_{N, T} = -k_{\text{B}}T (\ln q - \ln \theta) \quad (\text{S12})$$

Both of these models diverge in the identical way in the zero coverage limit, as in this limit the accessible area per adsorbate, and thus the number of states, goes to infinity in both. Both further behave identically in the low coverage limit, where the probability of two adsorbates occupying the same site vanishes and where the free energy is controlled by  $\ln q$ . At finite coverage, they differ according to whether an adsorbate excludes a particle from a site volume or not. Neither model is strictly “correct” at finite coverage, as both neglect adsorbate-adsorbate interactions. One or the other may be more satisfactory. Again, we focus here on the local site contributions to the chemical potentials, given by the  $\ln q$  expression.

## S2 Harmonic Oscillator fits to Z-direction PES

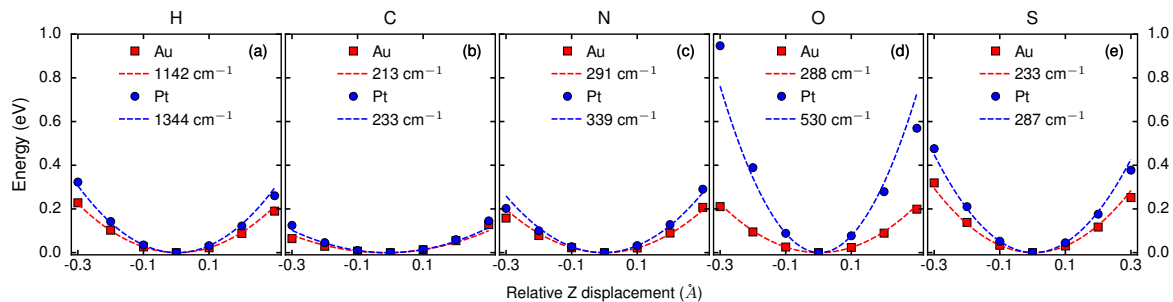


**Figure S1:** Harmonic oscillator fits to the potential energy variation along the z-coordinate. Energies are referenced to the energy minima for the respective adsorbate/metal system.

Figure S1 depicts harmonic oscillator fits for the z direction energy profile for all the adsorbate/metal(100) cases considered in this work. The vibration wavenumbers are higher for Pt(100) as compared to Au(100), indicating stronger binding strength of Pt.

## S3 Group 1: Four-fold adsorption, high diffusion barrier

### S3.1 N/Au

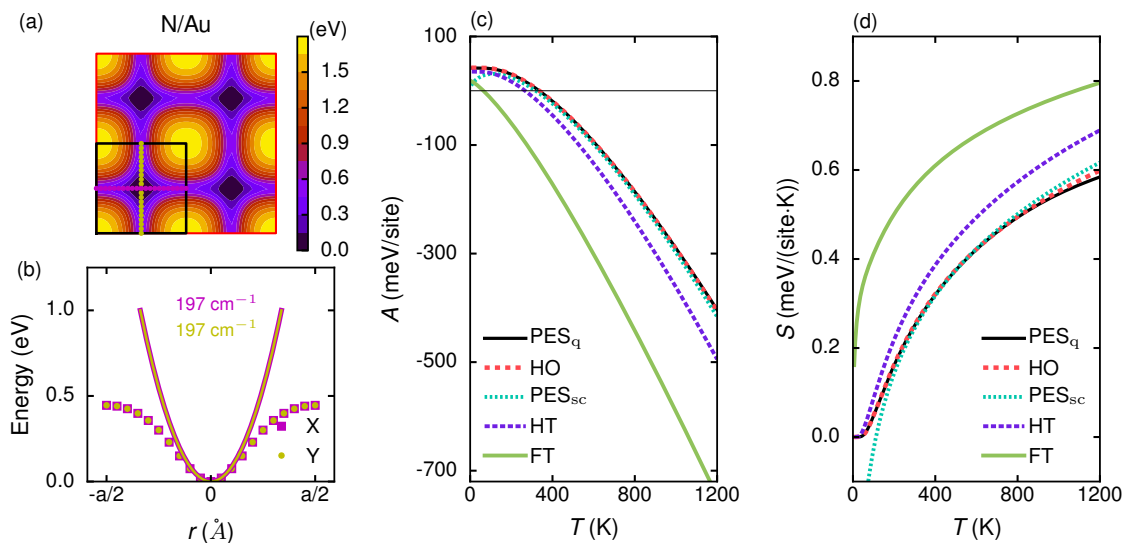


**Figure S2:** (a) In-plane N/Au PES. Magenta and yellow markers on the supercell grids depict the in-plane normal modes for adsorbate vibration. (b) Potential energy and harmonic fits along the normal vibration modes of the adsorbate. (c) Helmholtz free energy vs temperature and (d) Entropy vs temperature for five models: first-principles PES sampling ( $\text{PES}_q$ ), harmonic oscillator (HO), semi-classical PES sampling ( $\text{PES}_{sc}$ ), hindered translator (HT) and free translator (FT). Energies are referenced to the energy minima for the N/Au system.

## S3.2 S/Au

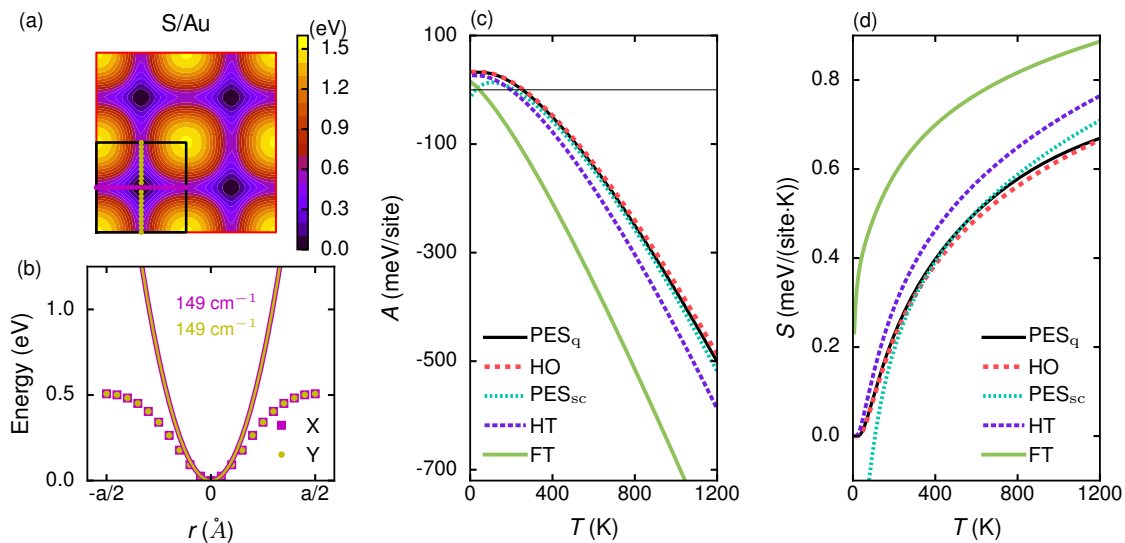


**Figure S3:** (a) In-plane S/Au PES. Magenta and yellow markers on the supercell grids depict the in-plane normal modes for adsorbate vibration. (b) Potential energy and harmonic fits along the normal vibration modes of the adsorbate. (c) Helmholtz free energy vs temperature and (d) Entropy vs temperature for five models: first-principles PES sampling (PES<sub>q</sub>), harmonic oscillator (HO), semi-classical PES sampling (PES<sub>sc</sub>), hindered translator (HT) and free translator (FT). Energies are referenced to the energy minima for the S/Au system.

### S3.3 C/Pt

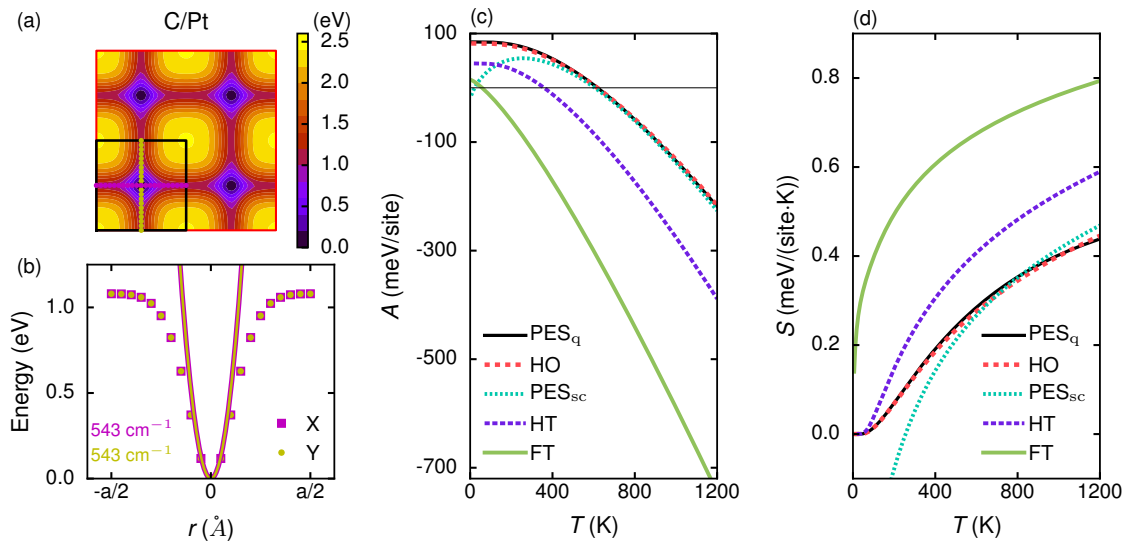


**Figure S4:** (a) In-plane C/Pt PES. Magenta and yellow markers on the supercell grids depict the in-plane normal modes for adsorbate vibration. (b) Potential energy and harmonic fits along the normal vibration modes of the adsorbate. (c) Helmholtz free energy vs temperature and (d) Entropy vs temperature for five models: first-principles PES sampling (PES<sub>q</sub>), harmonic oscillator (HO), semi-classical PES sampling (PES<sub>sc</sub>), hindered translator (HT) and free translator (FT). Energies are referenced to the energy minima for the C/Pt system.

### S3.4 S/Pt

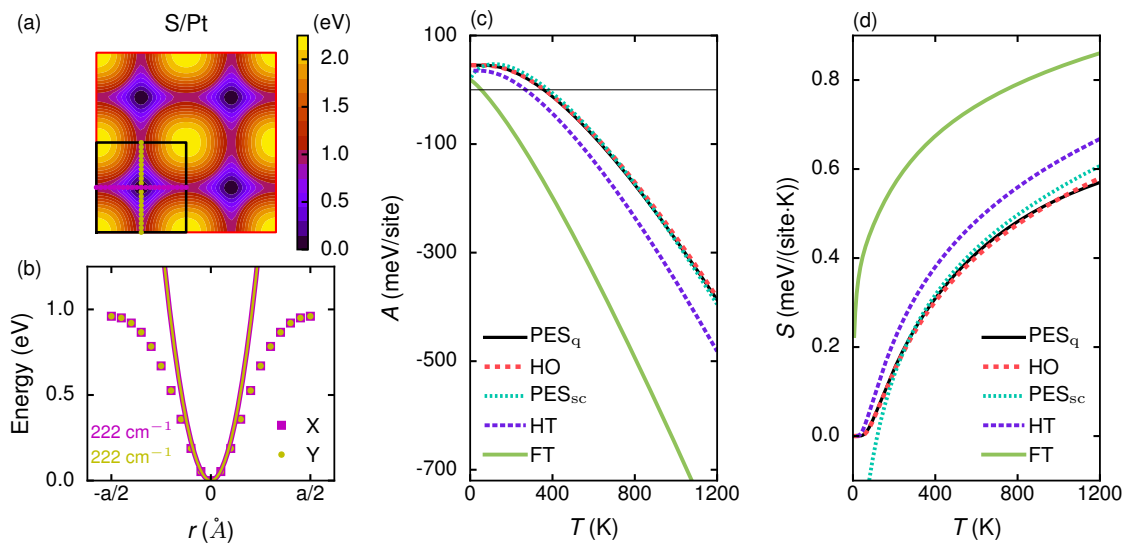


**Figure S5:** (a) In-plane S/Pt PES. Magenta and yellow markers on the supercell grids depict the in-plane normal modes for adsorbate vibration. (b) Potential energy and harmonic fits along the normal vibration modes of the adsorbate. (c) Helmholtz free energy vs temperature and (d) Entropy vs temperature for five models: first-principles PES sampling (PES<sub>q</sub>), harmonic oscillator (HO), semi-classical PES sampling (PES<sub>sc</sub>), hindered translator (HT) and free translator (FT). Energies are referenced to the energy minima for the S/Pt system.

## S4 Group 2: Four-fold adsorption, low diffusion barrier

### S4.1 N/Pt

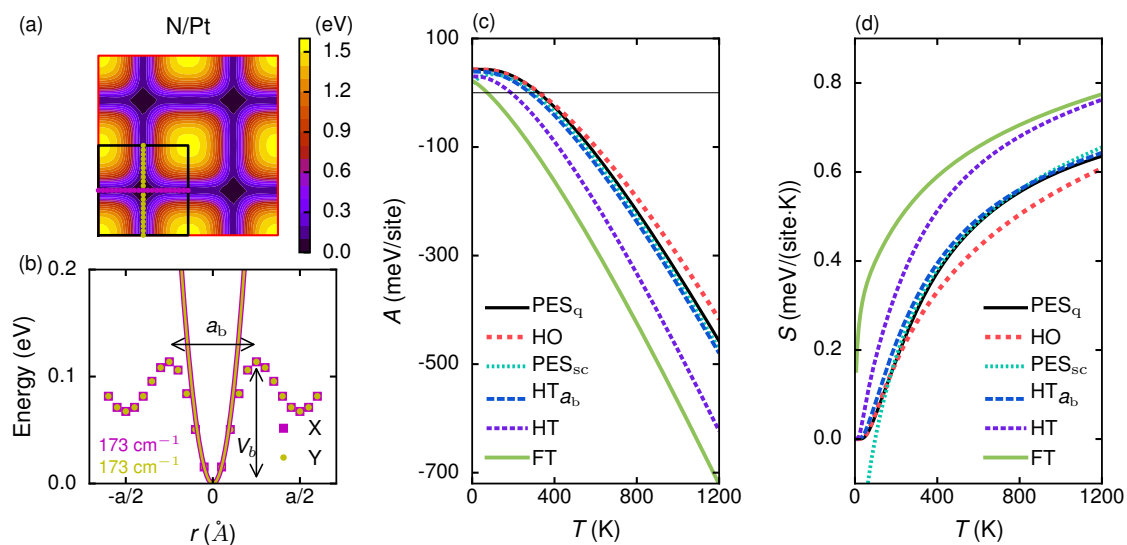


**Figure S6:** (a) In-plane N/Pt PES. Magenta and yellow markers on the supercell grids depict the in-plane normal modes for adsorbate vibration. (b) Potential energy and harmonic fits along the normal vibrational coordinates of the adsorbate. (c) Free energy vs temperature and (d) Entropy vs temperature for six models: first-principles PES sampling ( $\text{PES}_q$ ), harmonic oscillator (HO), semi-classical PES sampling ( $\text{PES}_{sc}$ ), hindered translator (HT), hindered translator with correction ( $\text{HT}_{ab}$ ), and the free translator (FT). Energies are referenced to the energy minima for the N/Pt system.

## S5 Group 3: Bridge site adsorption

### S5.1 H/Au

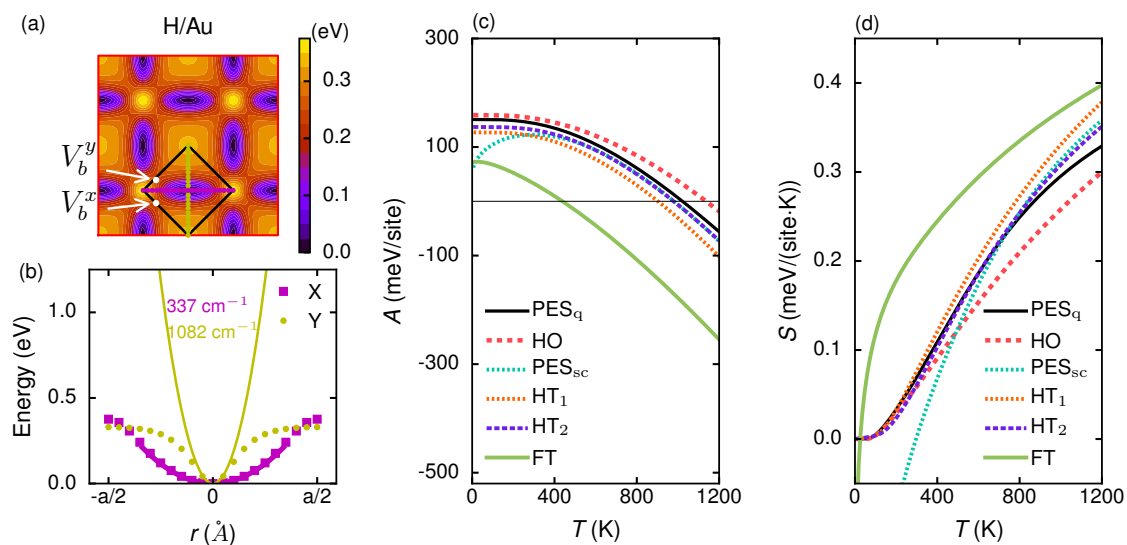


**Figure S7:** (a) In-plane H/Au PES. Magenta and yellow markers on the supercell grids depict the in-plane normal modes for adsorbate vibration. (b) Potential energy and harmonic fits along the normal vibration modes of the adsorbate. (c) Helmholtz free energy vs temperature and (d) Entropy vs temperature for five models: first-principles PES sampling (PES<sub>q</sub>), harmonic oscillator (HO), semi-classical PES sampling (PES<sub>sc</sub>), hindered translator (HT<sub>1</sub> and HT<sub>2</sub>) and free translator (FT). Energies are referenced to the energy minima for the H/Au system.

## S5.2 H/Pt

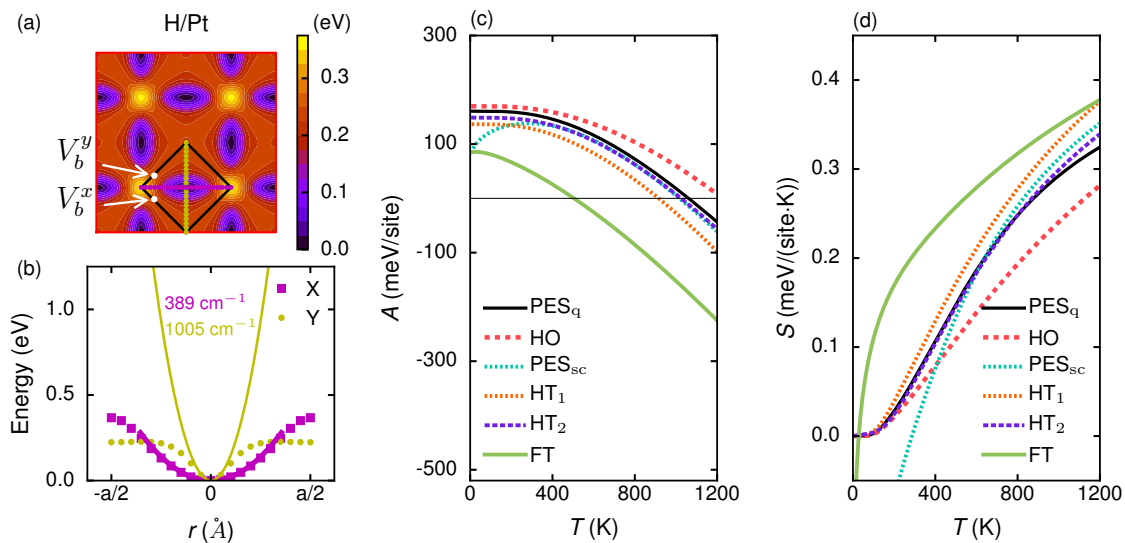


**Figure S8:** (a) In-plane H/Pt PES. Magenta and yellow markers on the supercell grids depict the in-plane normal modes for adsorbate vibration. (b) Potential energy and harmonic fits along the normal vibration modes of the adsorbate. (c) Helmholtz free energy vs temperature and (d) Entropy vs temperature for five models: first-principles PES sampling ( $\text{PES}_q$ ), harmonic oscillator (HO), semi-classical PES sampling ( $\text{PES}_{sc}$ ), hindered translator ( $\text{HT}_1$  and  $\text{HT}_2$ ) and free translator (FT). Energies are referenced to the energy minima for the H/Pt system.

## S6 PES solution for 3X3 supercell: O/Au system

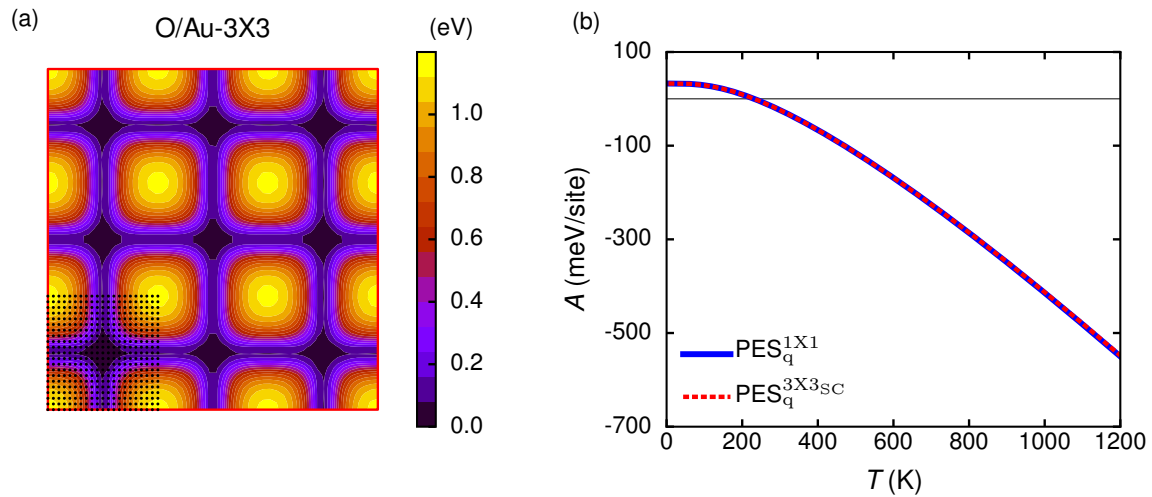


**Figure S9:** (a) Potential energy profiles for  $1\times 1$  and  $3\times 3$  supercell. (b) A comparison of area normalized Helmholtz free energy as a function of temperatures for  $1\times 1$  and  $3\times 3$  supercells.

## S7 Density of States

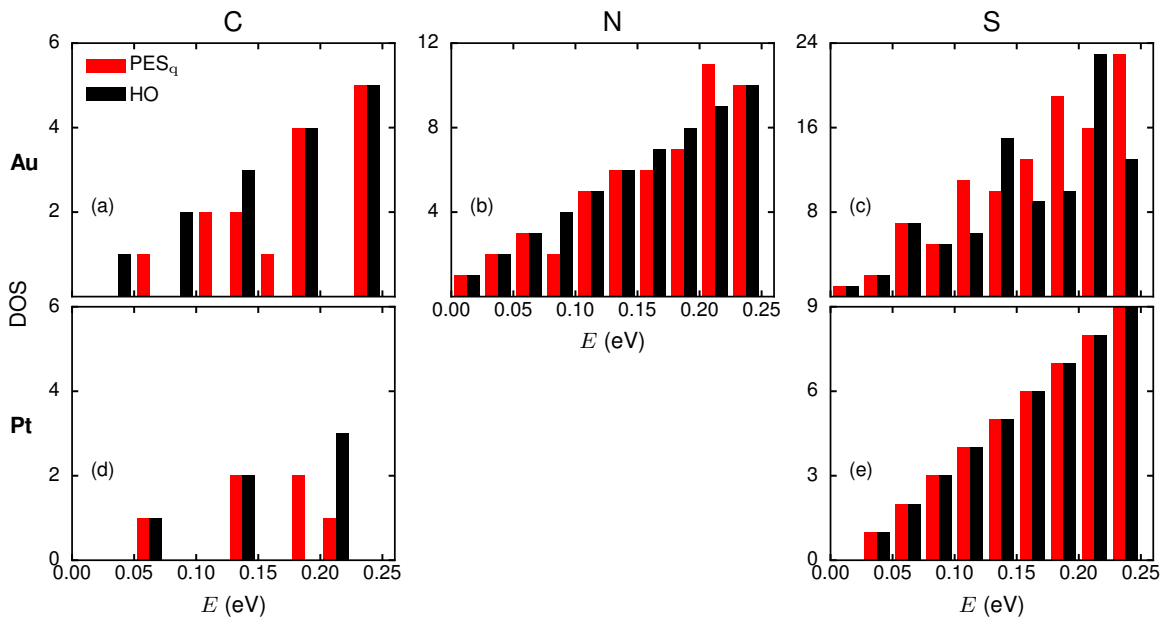


**Figure S10:** Histogram of energy solutions of in-plane energy states for (a) C/Au, (b) N/Au, (c) S/Au, (d) C/Pt, and (e) S/Pt systems.

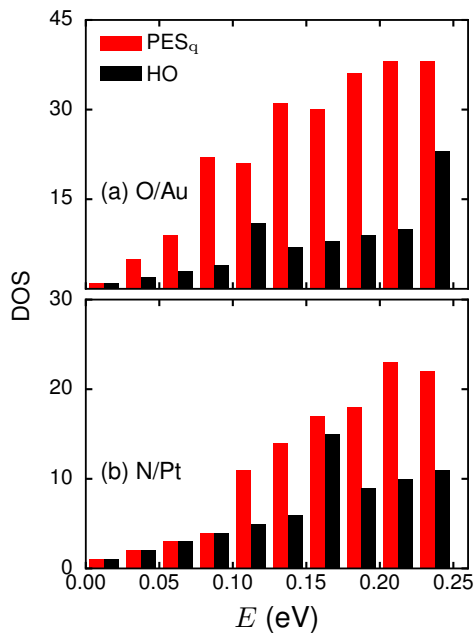


**Figure S11:** Histogram of energy solutions of in-plane energy states for (a) O/Au, and (b) N/Pt systems.

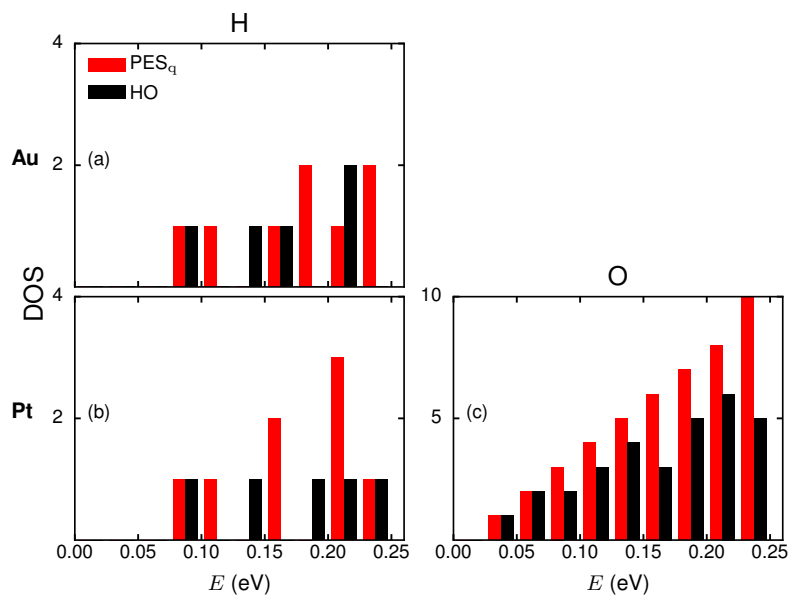


**Figure S12:** Histogram of energy solutions of in-plane energy states for (a) H/Au, (b) H/Pt, and (c) O/Pt systems.

## S8 Free Energy Estimates

**Table S1:** Helmholtz free energies (meV/site) at 100/500/1200 K for the systems considered in this work using different free energy models.  $HT_{ab}$  values are only for the group 2 cases with a two well potential energy profile.

Ads/Met	PES <sub>q</sub>	HO	HT	HT <sub>ab</sub>	FT
Group 1					
C/Au	64/-3/-294	63/-3/-289	38/-65/-435	—/—/—	-16/-240/-763
N/Au	41/-54/-403	41/-54/-406	33/-87/-495	—/—/—	-13/-233/-748
S/Au	30/-93/-501	30/-89/-487	21/-127/-588	—/—/—	-24/-281/-870
C/Pt	84/32/-219	81/31/-217	44/-45/-389	—/—/—	-14/-231/-743
S/Pt	44/-46/-387	44/-44/-383	33/-85/-482	—/—/—	-20/-267/-836
Group 2					
O/Au	29/-115/-550	37/-69/-440	11/-189/-703	21/-145/-598	-14/-239/-764
N/Pt	42/-67/-458	41/-59/-417	22/-144/-623	36/-84/-480	-9/-221/-721
Group 3					
H/Au	151/122/-56	159/135/-18	137/111/-72	—/—/—	77/2/-227
H/Pt	161/133/-44	170/149/8	149/122/-57	—/—/—	91/20/-196
O/Pt	68/-12/-329	68/-2/-290	52/-44/-401	—/—/—	9/-174/-612